ACS APPLIED MATERIALS & INTERFACES

Research Article

www.acsami.org

Enhanced Self-Assembly of Crystalline, Large-Area, and Periodicity-Tunable TiO_2 Nanotube Arrays on Various Substrates

Xiaoguang Liang,[†,⊥] Heng Zhang,[†] Ho-Wa Li,[†] Lei Shu,[†,⊥] HoYuen Cheung,[‡,⊥] Dapan Li,[†,⊥] SenPo Yip,[†,§,⊥] Qing Dan Yang,[†] Chun-Yuen Wong,[‡,§,⊥] Sai-Wing Tsang,[†,⊥] and Johnny C. Ho*[,†,§,⊥,∥]

[†]Department of Physics and Materials Science, [‡]Department of Biology and Chemistry, [§]State Key Laboratory of Millimeter Waves, and [∥]Centre for Functional Photonics, City University of Hong Kong, 83 Tat Chee Avenue, Kowloon Tong, Kowloon, Hong Kong

[⊥]Shenzhen Research Institute, City University of Hong Kong, 518057 Shenzhen, People's Republic of China

Supporting Information

ABSTRACT: Due to their superior physical properties, titanium dioxide (TiO_2) nanotube arrays are one of the most investigated nanostructure systems in materials science until now. However, it is still a great challenge to achieve damage-free techniques to realize controllable, cost-effective, and high-performance TiO_2 nanotube arrays on both rigid and flexible substrates for different technological applications. In this work, we demonstrate a unique strategy to achieve self-assemble crystalline, large-area, and regular TiO_2 nanotube arrays on various substrates via hybrid combination of conventional semiconductor processes. Besides the usual applications of TiO_2 as carrier transport layers in thin-film electronic devices, we demonstrate that the periodic TiO_2 nanotube arrays can show the effect of optical grating with large-area uniformity. Specifically, the fabricated nanotube geometries, such as the tube height, pitch, diameter, and wall thickness, as well as the crystallinity can be reliably controlled by varying the processing conditions. More importantly, utilizing these nanotube arrays in perovskite solar cells can further enhance the optical absorption, leading to improved power conversion efficiency. In contrast to other typical template-assisted fabrication approaches, we employ a soft template here, which would enable the construction of nanotube arrays without any significant damage associated with template removal. Furthermore, without the thermal restriction of underlying substrates, these crystalline nanotube arrays can be transferred to mechanically flexible substrates by a simple one-step method, which can expedite these nanotubes for potential utilization in other application domains.

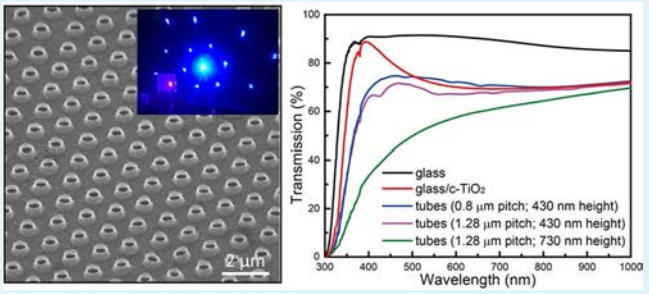

KEYWORDS: *titanium dioxide, nanotube, anatase, flexible substrate, optical grating, perovskite solar cell*

INTRODUCTION

In recent decades, due to its superior chemical stability, environmental friendliness, excellent electrical properties, and exceptional photoelectrical characteristics, titanium dioxide (TiO_2) has been considered as one of the most important transition-metal oxides.[1] For example, TiO_2 is a promising active material for many applications such as sensors,[2] dye-sensitized solar cells (DSSCs),[3] water splitting,[4,5] and other photovoltaic devices.[6,7] Various TiO_2 nanostructures with different geometrical morphologies, including nanoparticles,[8] nanorods,[9,10] nanotubes,[11] and others,[12,13] have also been successfully demonstrated as efficient light-absorbing electrodes with enhanced photoactivity in artificial photosynthesis[14−17] as well as effective electron-transporting layers (ETLs) with surprising optical transparency in organometal halide perovskite (e.g., $CH_3NH_3PbI_3$) devices.[7,18] Among all these nanostructures, TiO_2 nanotubes exhibit many extraordinary properties due to their excellent one-dimensional electron diffusion paths, unique optical grating, and light-harvesting capabilities, making them particularly useful in photoelectrochemical (PEC) and solar cell systems.[7,19−24]

In general, the synthesis of TiO_2 nanotubes can be accomplished by a wide variety of methods, namely, hydrothermal,[25] anodic self-organization,[26,27] template-assisted techniques,[28] and so on. Hydrothermal reaction approaches usually lead to a loose stacking of individual tubes lying randomly on the substrate, resulting in nanotubes with arbitrary orientations and consequently eliminating their advantage to possess one-dimensional diffusion paths.[29] On the other hand, the self-organizing anodization scheme can yield an alternative, simple, and low-cost route to prepare TiO_2 nanotube arrays by putting pure Ti foils under dilute fluoride electrolytes and controlled voltages.[5,11] In this case, although the tube geometries (i.e., length and tube diameter) are highly controllable in the large scale, the geometrical structure of these obtained tubes would

Received: September 30, 2016
Accepted: February 1, 2017
Published: February 1, 2017

DOI: 10.1021/acsami.6b12474
ACS Appl. Mater. Interfaces 2017, 9, 6265−6272

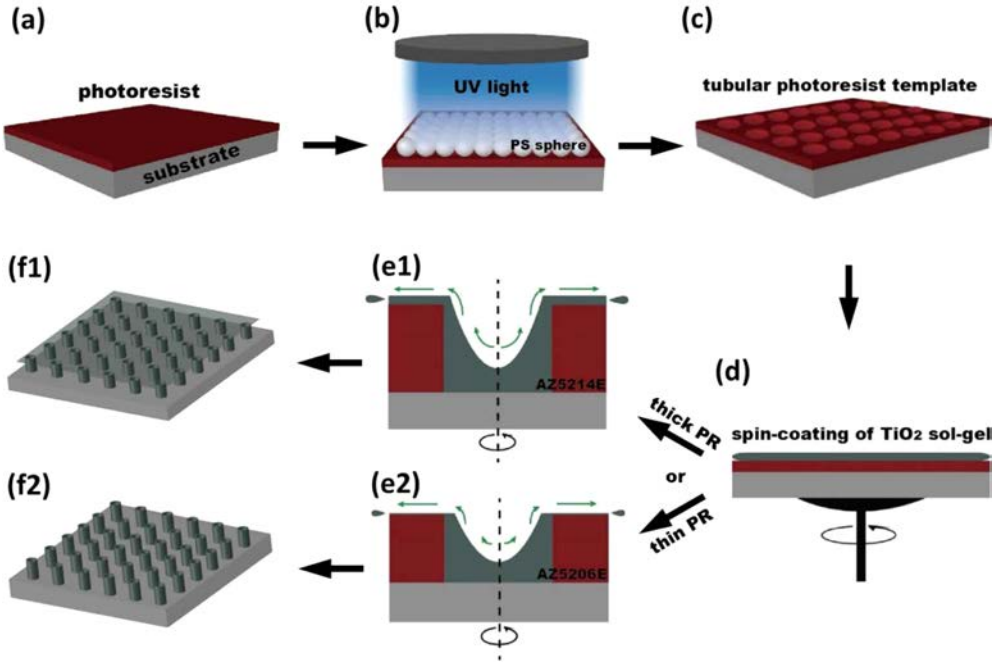

Figure 1. Schematic illustration of self-assembly of highly ordered TiO_2 nanotube arrays. (a) Substrate spin-coated with photoresist. (b) UV flood exposure on polystyrene (PS) sphere monolayer predeposited on the substrate. (c) Tubular hole features generated on photoresist as the fabrication template after PS sphere removal. (d) Template dip-coated with TiO_2 sol–gel and subsequently spin-dried. (e) Formation of a TiO_2 nanotube in the tubular hole of (e1) thick photoresist (AZ5241E) and (e2) thin photoresist (AZ5206E). (f) Nanotube arrays fabricated with the template of (f1) thick photoresist, with the top tips connected with a residual thin film layer after the resist lift-off, and (f2) thin photoresist after the resist lift-off.

leave interunit spacing of only several or tens of nanometers for the loading of light absorbers or hole transporting materials, which degrades the performance of subsequently fabricated devices.[30] Moreover, anodic aluminum oxide (AAO), silicon dioxide (SiO_2), and polycarbonate (PC),[26] etc., can be easily patterned as tubular structures on rigid substrates, and then they can be employed as templates for the deposition of TiO_2 nanotube arrays via sol–gel processes,[31,32] atomic layer deposition (ALD),[33] and sputtering.[34] However, the successive template removal steps would inevitably require harsh chemical etching, inducing significant issues of substrate delamination and substrate surface and tube wall damage, as well as tube aggregation.[35] At the same time, achieving these nanotube arrays with decent crystallinity on unconventional substrates (e.g., mechanically flexible plastics) can potentially extend their practical uses to other low-cost and portable application domains.[36,37] As a result, even with the restriction imposed by the underlying substrates, it is essential to develop damage-free and large-scale techniques to realize controllable, cost-effective, and high-performance TiO_2 nanotube arrays on both rigid and flexible substrates for different technological applications.

Recently, we have developed a rapid and large-scale nanopatterning scheme on different substrates by utilizing photoresist templates as soft masks.[38,39] Here, we further employ these nanopatterns as the template for self-assembly of crystalline, large-area, and periodicity-tunable anatase TiO_2 nanotube arrays on different surfaces. Since organic materials are used as templates, after the sol–gel deposition of nanotubes, only soft chemical processes are needed to dissolve the templates in order to preserve the tube properties without any of the above-mentioned damage. In this way, the fabricated tube geometries, such as height, pitch, diameter, and wall thickness, can be reliably controlled by varying the sol–gel precursor concentration, photoresist materials, and diameters of colloidal nanospheres. To illustrate the versatility of this self-assembly technique, we fabricate nanotube arrays with precisely tailored optical properties as well as superior light-trapping characteristics. Specifically, methylammonium lead iodide ($CH_3NH_3PbI_3$) perovskite thin film can be successfully spin-coated onto the nanotube arrays, resulting in improved optical absorption, leading to higher power conversion efficiency of the subsequently fabricated solar cell device as compared with its planar counterpart. More importantly, as contrasted with other soft-template-assisted approaches,[40] these highly crystalline nanotube arrays can also be readily transferred onto other flexible substrates due to the unique assembly characteristics. All of these not only demonstrate the low-cost, facile, and scalable construction of TiO_2 nanotube arrays on various substrates but also provide an exciting platform for different technologies, especially in the area of photovoltaics.

EXPERIMENTAL SECTION

Precursor and Substrate Materials. Titanium(IV) isopropoxide (98%, J&K) was used to fabricate the titania compact layer (c-TiO_2) and the titania sol–gel precursor. Then we designed and employed six different functional substrates in this work: (i) Si, (ii) fluorine-doped tin oxide (F:SnO_2, FTO) coated glass (10 Ω/sq), (iii) standard glass slides coated with a c-TiO_2 thin layer (Si/c-TiO_2, FTO/c-TiO_2, and glass/c-TiO_2), (iv) indium tin oxide-coated poly(ethylene terephthalate) (PET/ITO) with ITO thickness of 0.175 mm and sheet resistance of 25 Ω/sq, and (v) polyimide (PI) as well as (vi) bare single-crystalline p-type (100) Si wafers (bare Si). The substrates PET/ITO, bare Si, FTO/c-TiO_2, and glass were rinsed in succession by deionized (DI) water, acetone, and ethanol for 15 min with ultrasonication and next were subjected to mild oxygen plasma treatment under a process pressure of 0.26 Torr with a power of 30 W for 5 min. Then, a 50 nm thick TiO_2 compact layer was synthesized by spin-coating titanium isopropoxide solution (i.e., 730 μL of titanium

DOI: 10.1021/acsami.6b12474
ACS Appl. Mater. Interfaces 2017, 9, 6265–6272

isopropoxide diluted in 5 mL of ethanol, and then 69 μL of 2 M HCl was added into the mixture) on Si and glass surfaces at 2000 rpm for 60 s. TiO_2-coated samples were then calcined at 500 °C for 30 min in air.

Template Fabrication. Photoresist layers with different thickness (i.e., AZ5214E, 1 μm thick, and AZ5206E, 460 nm thick) were spin-coated on the substrates at 5000 and 4000 rpm for 60 s, respectively, with a 15 min soft baking at 90 °C for Si and 100 °C for glass. Before spin-coating of the photoresist, all substrates were baked at 120 °C for 20 min to evaporate all water molecules adhered on the surface. By use of the Langmuir−Blodgett (LB) method, polystyrene (PS) nanospheres of 1.27 and 0.8 μm diameter were assembled on the photoresist films as a close-packed monolayer.[39] Next, the samples were irradiated by UV illumination for 3 s (AZ 5214E) or 2 s (AZ 5206E), via the flood exposure mode in a SUSS MicroTec mask aligner (MA/BA6). After UV illumination, the PS spheres were removed by ultrasonication in DI water and the exposed samples were developed in AZ-300 MIF developer, followed by a DI water rinse. Subsequently, with the nitrogen blow-dry, the photoresist templates with tubular holes were fabricated. In order to eliminate the residual photoresist at the hole bottom, all substrates were treated with another mild oxygen plasma at 0.26 Torr with a power of 30 W for 10 s.

TiO_2 Sol−Gel Materials. Since the photoresist would be easily dissolved in organic solvents such as acetone and ethanol, titanium aqueous solution acidified with nitric acid was selected as the precursor here. In brief, 8 mL of titanium isopropoxide was added into 100 mL of DI water acidified with 0.7 mL of nitric acid (68−70%). The mixture was first started from the white suspension and subsequently peptized at 85 °C with vigorous stirring in an open Erlenmeyer flask for about 12 h until a volume of 27 mL was obtained.[41] The final colloids of less than 15 nm formed a translucent solution, stabilized by adjusting the water-to-titanium mole ratio of ∼120 and 200 through addition of DI water droplets. This process facilitates the formation of crystalline nanotube arrays along with precise control of the obtained tube thickness. Unless otherwise stated, the TiO_2 sol−gel material with a water-to-titanium mole ratio of 200 was mainly employed in this study.

TiO_2 Nanotube Array Fabrication. At first, the finished templates were immersed into the TiO_2 sol−gel solution for 10 s, and then they were spin-coated at 4000 rpm for 30 s in order to reduce the excessive TiO_2 on top of the photoresist. After they were baked at 60 °C for 10 min, the samples were rinsed in ethanol to dissolve the photoresist, followed by a DI water rinse and nitrogen blow-dry. To enhance the crystallization of attained TiO_2 nanotubes, the samples were then annealed at 500 °C for 30 min in air. It is also noted that titania thin film (several nanometers thick) connecting the tips of nanotubes was observed for the thick resist samples (AZ5214E, Figure 1f1), where this thin film would be performed as the enabling feature for subsequent transfer of these nanotube arrays onto other plastic substrates; details will be described under Results and Discussion. When necessary, this top thin film can be removed by plasma etching with a power of 100 W and a process argon pressure of 0.19 Torr for 2 min.

Characterization. Geometrical morphologies of the fabricated photoresist templates and TiO_2 nanotube arrays were assessed by scanning electron microscopy (SEM, Quanta FEG450). X-ray diffraction (XRD, SmartLab X-ray diffractometer, Cu Kα radiation, λ = 1.5406 Å) and Raman spectroscopy (Renishaw inVia Raman Microscope) were used to evaluate the crystal structure of titania tubes. For the titania nanotubes on glass/c-TiO_2 substrates, detailed optical properties were measured via ultraviolet−visible (UV−vis) spectrophotometry (PerkinElmer Lambda 2S UV/vis spectrometer).

RESULTS AND DISCUSSION

The process schematic of this newly developed self-assembly technique of highly ordered TiO_2 nanotube arrays is depicted in Figure 1, in which the photoresist layer prepatterned with controllable tubular features is used as the fabrication template (Figure 1a−c). The template is first dipped into the titania sol−gel solution for a short time and processed with a spin-coating step immediately (Figure 1). This spin-coating condition together with the photoresist thickness and sol−gel concentration are critical in directly reducing or completely removing the excessive titania floating on top of the template as well as precisely controlling the amount of titania to fill the tubular holes for the nanotube formation. Specifically, photoresist layers with two different thicknesses (AZ5206E, 460 nm, and AZ5214E, 1 μm) are selected in this work for self-assembly of TiO_2 nanotubes (Figure 1d). It is found that titania nanoparticles in the sol−gel solution are typically nucleated around the surface of the photoresist pattern, resulting in the tubular structure instead of the pillar configuration. When samples with different resist thicknesses are compared (Figure 1e), there is always a residual thin-film layer covering the space of the nanotube arrays in samples with the thicker resist (AZ5214E). Formation of this film can be attributed to larger quantities of colloids confined in larger volumes of tubular holes after dip-coating, yielding excessive amounts of titania particles adhered on top of the resist surface and subsequently leaving a residual film after the resist lift-off. It is also worth noting that formation of these TiO_2 tubular topographies and top surface thin films is independent of the sol−gel concentration as well as the spin-coating condition, as indicated in Figure S1. Surprisingly, these residual films could act as an enabling feature to facilitate the successive transfer of these nanotube arrays onto other substrates, extending their practical applications. The details will be discussed later. If necessary, these residual films can be completely etched away and removed with a mild argon plasma treatment after spin-coating in order to accomplish the establishment of nanotube arrays.

Generally, the predominant advantage of utilizing these photoresist-based templates is that the nanotube arrays can be synthesized on various substrate surfaces with tunable geometrical parameters in the large scale, together with damage-free template removal characteristics. Simply by varying the size of polystyrene (PS) spheres in the prior self-assembled nanosphere photolithographic step, tubular hole patterns with a pitch ranging from 1.28 μm all the way to 800 nm can be readily obtained on the photoresist layer with a thickness of 460 nm (AZ5206E) as displayed in Figure 2a,b. The exact same pattern can also be achieved on the thicker photoresist layer (AZ5214E, 1 μm thickness) as depicted in Figure 2c. All these tubular hole pattern dimensions, including pitch, diameter, and height, would in principle dictate the size of subsequently assembled nanotube arrays. Notably, when the thickness of photoresist template layers increases, the light-focusing nature of PS spheres would generate a nonuniform exposure profile across the depth of the resist layer, inducing a drum-shaped tubular hole feature there.[39] Specifically, Figure 2d illustrates the successful self-assembly of highly ordered TiO_2 nanotube arrays with tube height of 430 nm, external tube diameter of 420 nm, and pitch of 1.28 μm on bare Si substrates after sintering at 500 °C for 30 min in air. As compared with the initial photoresist template thickness of 460 nm (AZ5206E), this slightly reduced tube height of 430 nm is probably due to the combination of resist lift-off in ethanol, DI water rinse, and pattern shrinkage after the assembly process. Since many applications require a compact seed layer underneath the TiO_2 nanotube arrays (e.g., perovskite solar cells), we also assembled well-ordered titania nanotube arrays on Si/c-TiO_2 substrates as demonstrated in Figure 2e. It is noted that the dimensional uniformity of these nanotubes is not as good as the ones

DOI: 10.1021/acsami.6b12474
ACS Appl. Mater. Interfaces 2017, 9, 6265−6272

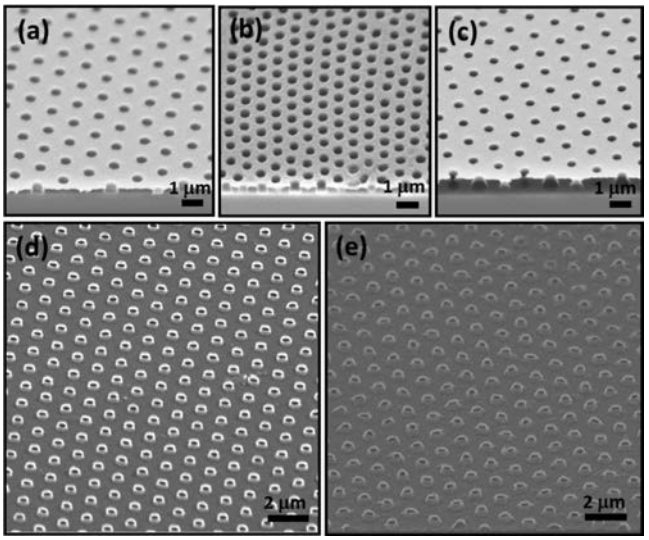

Figure 2. Scanning electron microscopic (SEM) images of photoresist patterns and TiO_2 nanotube arrays obtained in this self-assembly process. (a, b) Tubular hole features patterned with a pitch of (a) 1.28 μm and (b) 800 nm (AZ5206E, 460 nm in thickness). (c) Tubular hole features patterned with a pitch of 1.28 μm (AZ5214E, 1 μm in thickness). (d, e) TiO_2 nanotube arrays self-assembled onto (d) bare silicon substrate and (e) silicon substrate predeposited with titania compact layer (Si/c-TiO_2). Both employ AZ5206E photoresist templates with pitch of 1.28 μm and feature thickness of 460 nm.

fabricated on bare Si substrates. This can be attributed to the nonconformal coating of underlying seed layers, which induce somewhat distorted tubular templated features for tube assembly. We expect that the geometrical uniformity of these nanotubes will be improved once these seed layers become conformal. Because of the practical requirement of many technological device configurations, unless otherwise stated, Si/c-TiO_2 substrates are typically employed in the rest of this study.

Up to now, owing to technological constraints, apart from anodization schemes, more and more works have been focused on the construction of TiO_2 nanotube arrays via direct growth techniques and soft-template-assisted approaches. However, it is still challenging to reliably control the pitch and size of fabricated tube arrays due to the random nature of direct growth as well as the complicated lithographic processes employed in template manufacture.[30,40] In this work, by just employing different dimensions of PS spheres, geometrical parameters of the titania nanotube arrays can be readily manipulated. As shown in Figure 3a, TiO_2 nanotube arrays with pitch of 0.8 μm, external tube diameter of 290 nm, and tube height of 430 nm are successfully attained. More importantly, the tube height and wall thickness can also be precisely tuned by varying the thickness of photoresist templates utilized and the precursor sol–gel concentration, respectively. For instance, when a 1 μm thick resist template (AZ5214E) is used, the tube height can then be increased to 730 nm as depicted in Figure 3b. As discussed earlier, residual titania thin films connecting the tips of the tubes are always formed when the thicker template is used; therefore, a mild argon plasma treatment can be used to remove these residual films. This way, combined with the post-assembly thermal annealing, the tube height would be decreased to some extent as compared with the starting template thickness, which is attributable to plasma etching of tube brims as well as tube shrinkage from solvent evaporation. At the same time, when sol–gel concentration

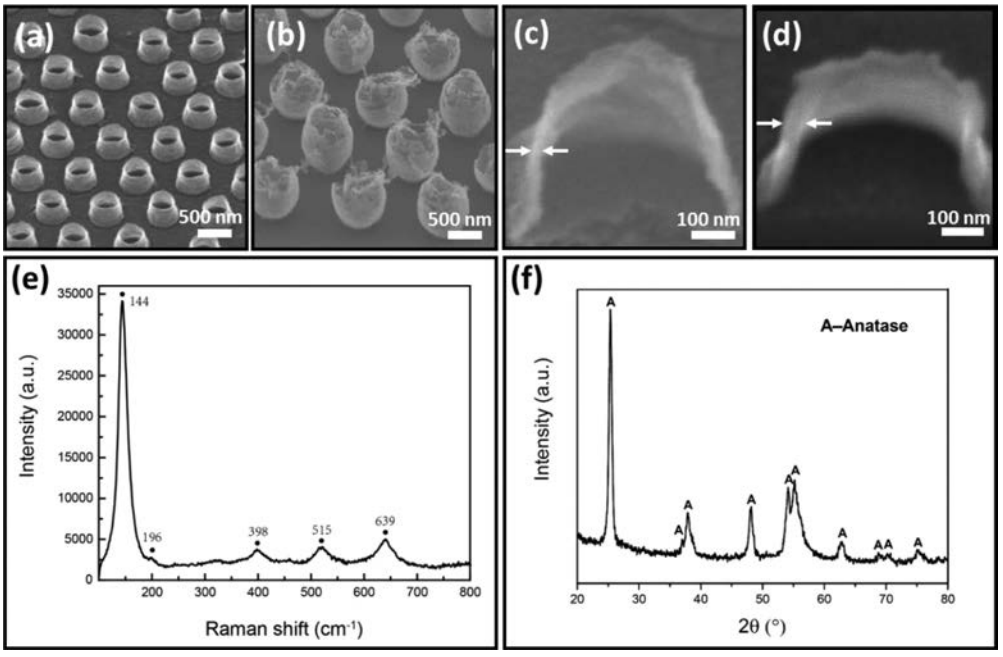

Figure 3. Characterization of assembled TiO_2 nanotube arrays. (a) SEM image of nanotube arrays with pitch 0.8 μm, fabricated with resist template thickness of 460 nm (AZ5206E). (b) SEM image of nanotube arrays with pitch 1.28 μm, fabricated with resist template thickness of 1 μm (AZ5214E). (c) Zoom-in SEM image of panel a, indicating tube wall thickness of about 25 nm, synthesized via sol–gel concentration with a water-to-titanium mole ratio of 200. (d) Zoom-in SEM image of panel b, indicating tube wall thickness of about 50 nm, synthesized via sol–gel concentration with a water-to-titanium mole ratio of 120. (e) Raman spectra and (f) grazing incidence XRD pattern of the representative titania nanotube arrays after thermal treatment. The selected sample structure for XRD is Si/c-TiO_2/TiO_2 nanotube arrays, in which the thickness of c-TiO_2 layer and TiO_2 nanotube arrays are 50 and 760 nm, respectively.

DOI: 10.1021/acsami.6b12474
ACS Appl. Mater. Interfaces 2017, 9, 6265–6272

with a water-to-titanium mole ratio of 200 and 120 is employed, tube wall thicknesses of 25 and 50 nm can be obtained, which are shown in SEM images in Figure 3c,d. Notably, since the PS spheres would yield nonuniform exposure characteristics along the depth of the resist layer during colloidal lithography, when the resist layer thickness is comparable to or larger than the size of PS spheres, spherical-shaped nanotubes will be formed (Figure 3b). Although the maximum achievable aspect ratio of these nanotubes is limited to around 2 in this work, the respectable variation of tube height, diameter, and pitch is sufficient for various crucial device applications.[30,42] In the future, different patterning techniques such as nanoimprinting can be further explored to achieve tubular hole features with higher aspect ratios for improved nanotube fabrication.

In addition, the crystal structure and material quality of titania nanotubes are known to have a significant effect on their electrical, optical, and photoelectrochemical properties. Among many phases, the non-equilibrium anatase structure is widely considered as the ideal phase of TiO_2 because of its relatively high electron mobility and superior electron injection velocity.[43] Both X-ray diffraction (XRD) and Raman spectroscopy are utilized to assess and evaluate the crystal phase and crystallinity of as-prepared TiO_2 nanotube arrays. Figure 3e presents the Raman spectrum of titania nanotubes obtained, ranging from 100 to 800 cm^{-1}. Four broad peaks are observed at 144, 398, 515, and 639 cm^{-1}, which confirms the formation of anatase phase. In particular, the intrinsically weak peak at 196 cm^{-1} is a distinctive feature of anatase TiO_2.[44] After the optimized post-assembly treatment, the XRD pattern of titania nanotubes is then shown in Figure 3f, indicating that the attained anatase titania nanotubes arrays display excellent crystal quality, suitable for devices with enhanced performance.

One of the unique characteristics of our soft-template-assisted self-assembly of TiO_2 nanotube arrays is that the entire fabrication scheme is not limited to conventional rigid substrates; it can also be extended to other non-standard substrates, such as poly(ethylene terephthalate) (PET) films, which is commonly used as a mechanical flexible substrate. However, typical organic-based flexible plastics cannot survive the relatively high temperatures, up to 500 °C, that are generally employed for calcination of TiO_2 nanotubes into the anatase phase. As depicted in Figure 4a,b, even though the regular titania nanotubes can be readily self-assembled onto PET substrates predeposited with a thin film layer of indium tin oxide (ITO) with well-controlled pitch and tube geometries, they still suffer from poor crystallinity due to the lack of a high thermal annealing step, restricted by the plastic substrate. The corresponding XRD pattern indicates that the as-prepared titania tubes are mostly amorphous, and so their electrical and photoelectrical properties are probably poor, making them unsuitable for any device applications. In this case, the distinctive formation of residual thin films connecting the tips of the tubes during the self-assembly would facilitate the simple one-step mechanical transfer of high-quality anatase nanotube arrays initially assembled on Si (i.e., mother substrate) onto any other foreign surface (i.e., donor substrate) (Figure 4c). For example, as outlined in Figure 4d, once the polyimide (PI) film is gently attached to the top surface of nanotube arrays fabricated on the rigid substrate, the residual thin film would then function as a good anchor to reinforce the interface interaction between the PI surface and the tube brims. The boundary between the tube bottom base and rigid substrate would then become a mechanically weak region. When the PI film is carefully peeled off, the anatase TiO_2 nanotube arrays can be easily transferred there in an inverted fashion without any geometrical distortion and degradation in the structural integrity (Figure 4e). It is also noted that after the transfer the residual film is located at the basal plane of the nanotube arrays, where it is advantageous to work as the compact seed layer for various device needs. Therefore, this simple one-step transfer approach, associated with our newly developed self-assembly of titania nanotube scheme, could be used as a versatile tool for the controllable fabrication of nanotube arrays on various substrates for a wide variety of uses.

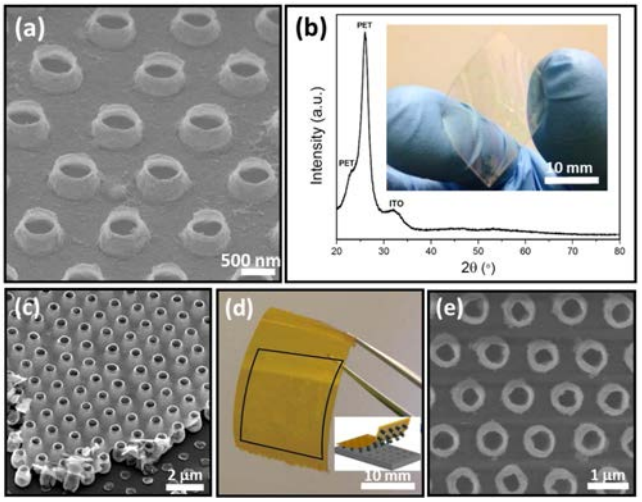

Figure 4. Well-ordered TiO_2 nanotube arrays assembled on mechanically flexible substrates. (a) SEM image of nanotube arrays fabricated on poly(ethylene terephthalate) substrates predeposited with a thin layer of indium tin oxide (PET/ITO), with pitch 1.28 μm, tube height 430 nm, and wall thickness 25 nm. (b) XRD pattern of corresponding nanotube arrays fabricated directly on PET/ITO substrates, indicating their poor crystallinity. (Inset) Optical image of the sample (20 × 30 mm^2), demonstrating its mechanical flexibility and optical transparency. (c) SEM image of nanotube arrays obtained with a residual thin film connecting the tips of each tube. The tube pitch is 1.28 μm and the tube height is 730 nm. (d) Photograph of nanotube arrays displayed in panel c after being mechanically transferred onto another polyimide (PI) substrate. (Inset) Schematic illustration of nanotube array transfer process. (e) Corresponding top-view SEM image of transferred nanotube arrays, demonstrating minimal post-transfer geometrical distortion and structural integrity degradation of nanotubes as well as the absence of any residual surface films.

To shed light on their optical properties for practical uses, highly ordered anatase TiO_2 nanotube arrays with different pitches and heights are fabricated on transparent glass substrates predeposited with a compact seed layer (glass/c-TiO_2), followed by the characterization with detailed diffraction and UV−vis spectroscopic measurements as indicated in Figure 5. Explicitly, the diffraction pattern of large-area TiO_2 nanotube arrays with tube height 430 nm and pitch 1.28 μm is shown in Figure 5a, confirming their high degree of periodic ordering. These periodic nanotube arrays possess the unique ability to harvest, guide, and trap light. For example, the optical characteristics (i.e., transmittance or absorption) can be tuned by varying the pitch and tube diameter of the arrays.[24,45] Figure 5a (inset) shows the optical image of a corresponding sample where the diffraction color indicates a long-range uniform distribution of nanotube arrays over the sample surface.

DOI: 10.1021/acsami.6b12474
ACS Appl. Mater. Interfaces 2017, 9, 6265−6272

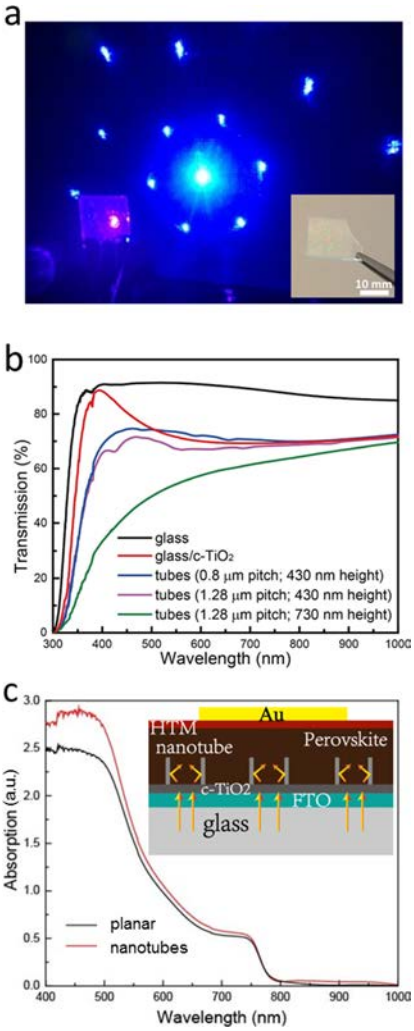

Figure 5. (a) Diffraction patterns of TiO_2 nanotube photonic crystal arrays assembled on glass/c-TiO_2 substrate with height 430 nm and pitch 1.28 μm, illuminated by a laser with wavelength 403 nm. (Inset) Photograph of corresponding sample. (b) Transmission characteristics of TiO_2 nanotube arrays assembled on glass/c-TiO_2 substrate with different heights and pitches. The normal incident wavelength range is between 300 and 1000 nm. (c) UV−vis absorption spectra of the perovskite layer spin-coated onto nanotube and planar substrates. (Inset) Enhanced optical absorption enabled by light trapping within nanotube arrays of subsequently fabricated solar cell devices.

Diffraction patterns for samples with different pitches and heights are also presented in Figure S2.

Figure 5b illustrates the dependence of optical transmission on different pitches and heights of the assembled titania nanotube arrays. It is expected that, with a constant tube height of 430 nm, when the tube pitch and diameter increase from 0.8 to 1.28 μm and 290 to 420 nm, respectively, the transmission is attenuated. At the same time, when the tube height increases from 430 to 730 nm, the transmission decreases for constant tube pitch and diameter of 1.28 μm and 420 nm, accordingly. Even for different tube pitches and diameters, the transmission is observed to be predominantly dependent on the tube height. In the region below the wavelength of 330 nm, TiO_2 nanotube arrays show a slight influence on transmission, due to the serious light absorption by glass and c-TiO_2 layers. The variation of transmittance is mainly observed in the visible wavelength region between 400 and 700 nm, in which the corresponding maximum difference is roughly 32% at the wavelength of 450 nm. Incident light is trapped in the interior of these TiO_2 nanotubes with different geometrical parameters, resulting in the variation of transmission in the visible range of 400 to 700 nm. However, the effect of geometry on light trapping becomes weaker over a spectral range for $\lambda > 700$ nm. Notably, measurements on bare glass and glass/c-TiO_2 samples are also performed to confirm that the obtained optical characteristics indeed result from the assembled nanotube arrays, especially since the transmission of glass/c-TiO_2 substrate is decreased significantly in the longer-wavelength range, probably caused by specular reflection associated with the relatively high refractive index of the compact layer there. Similarly, absorption characteristics of all the samples are estimated from transmittance and depicted in Figure S3, with consistent results attained. It should also be noted that simply by manipulating the tube pitch, diameter, and height of these nanotube arrays, their optical properties can be reliably controlled and designed for superior photon management electrodes for optoelectronic device applications, such as electron-transporting materials (ETM) in perovskite solar cells, as depicted in Figure 5c. Here, $CH_3NH_3PbI_3$ solution is spin-coated onto both planar (i.e., glass/FTO/c-TiO_2) and nanotube-arrayed (i.e., glass/FTO/c-TiO_2/TiO_2 nanotube) substrates by utilizing the one-step method (see Supporting Information for additional experimental details).[46] As compared with the planar-configured sample, the nanotube sample exhibits a significant improvement in optical absorption in the visible region, which can be attributed to the efficient light trapping enabled by the nanotube arrays here, as widely reported in the literature.[47] As a result, as compared with the conventional planar structure, the perovskite solar cell fabricated with the TiO_2 nanotube arrays has more than 20% improvement in the short-circuit current (J_{SC}), which is in good agreement with the enhanced light absorption as observed in UV−vis measurements. The corresponding current−voltage characteristics and device performance are as well summarized in Figure S4. In the future, once the device structures, including tube diameter, length, and tube/active layer interface properties, are optimized, we expect that the efficiency will be further elevated. Regardless, all these results have evidently demonstrated the versatility and technological potency of our self-assembled anatase titania nanotube arrays in photovoltaic applications.

CONCLUSIONS

In conclusion, a cost-effective and reliable soft-template-assisted fabrication approach is presented for the facile self-assembly of well-ordered and crystalline TiO_2 nanotube arrays on different types of substrate materials. By just manipulating the size and periodicity of template patterns associated with different colloid dimensions and lithographic conditions, the nanotube pitch, diameter, and height could be obtained in a highly controllable manner. Significantly, the formation of residual thin films connecting the tube brims during the self-assembly process can be utilized to enable the simple one-step transfer of these crystalline nanotube arrays onto mechanically flexible substrates. This way, high-quality nanotube arrays can be readily achieved on different unconventional surfaces without the thermal restriction of underlying substrates. At the same time, the excellent uniformity of these nanotube arrays is then further evaluated and confirmed with their geometry-dependent optical properties. Subsequent utilization of these nanotube arrays in

DOI: 10.1021/acsami.6b12474
ACS Appl. Mater. Interfaces 2017, 9, 6265−6272

perovskite solar cells can enhance the optical absorption, leading to improved power conversion efficiency. Obviously, this simple self-assembly technique could be further optimized as a general approach for the viable large-scale fabrication of regular nanotube arrays with other material systems, which could possibly facilitate practical applications of nanotube arrays in a wide range of potential technologies, including functional coatings and photovoltaics.

■ ASSOCIATED CONTENT

Supporting Information

The Supporting Information is available free of charge on the ACS Publications website at DOI: 10.1021/acsami.6b12474.

Additional text and four figures describing SEM images, diffraction patterns, and absorption characteristics of various nanotube arrays and perovskite solar cell fabrication details and corresponding photovoltaic characteristics (PDF)

■ AUTHOR INFORMATION

Corresponding Author

*E-mail johnnyho@cityu.edu.hk.

ORCID

Chun-Yuen Wong: 0000-0003-4780-480X

Johnny C. Ho: 0000-0003-3000-8794

Notes

The authors declare no competing financial interest.

■ ACKNOWLEDGMENTS

This research was financially supported by the General Research Fund (CityU 11213115) and the Theme-based Research Scheme (T42-103/16-N) of the Research Grants Council of Hong Kong SAR, China, the National Natural Science Foundation of China (Grant 51672229), the Science Technology and Innovation Committee of Shenzhen Municipality (Grant JCYJ20160229165240684), and the City University of Hong Kong (Grant 9667124). It was also supported by a grant from the Shenzhen Research Institute, City University of Hong Kong. We thank Professor Kin Man Yu for discussion.

■ REFERENCES

(1) Paramasivam, I.; Jha, H.; Liu, N.; Schmuki, P. A Review of Photocatalysis Using Self-Organized TiO_2 Nanotubes and Other Ordered Oxide Nanostructures. *Small* **2012**, *8*, 3073−3103.

(2) Zhu, Y.; Shi, J.; Zhang, Z.; Zhang, C.; Zhang, X. Development of a Gas Sensor Utilizing Chemiluminescence on Nanosized Titanium Dioxide. *Anal. Chem.* **2002**, *74*, 120−124.

(3) Sheng, X.; He, D.; Yang, J.; Zhu, K.; Feng, X. Oriented Assembled TiO_2 Hierarchical Nanowire Arrays with Fast Electron Transport Properties. *Nano Lett.* **2014**, *14*, 1848−1852.

(4) Wang, G.; Wang, H.; Ling, Y.; Tang, Y.; Yang, X.; Fitzmorris, R. C.; Wang, C.; Zhang, J. Z.; Li, Y. Hydrogen-Treated TiO_2 Nanowire Arrays for Photoelectrochemical Water Splitting. *Nano Lett.* **2011**, *11*, 3026−3033.

(5) Liu, Q.; He, J.; Yao, T.; Sun, Z.; Cheng, W.; He, S.; Xie, Y.; Peng, Y.; Cheng, H.; Sun, Y.; Jiang, Y.; Hu, F.; Xie, Z.; Yan, W.; Pan, Z.; Wu, Z.; Wei, S. Aligned Fe_2TiO_5-Containing Nanotube Arrays with Low Onset Potential for Visible-Light Water Oxidation. *Nat. Commun.* **2014**, *5*, No. 5122.

(6) Kim, H. S.; Lee, J. W.; Yantara, N.; Boix, P. P.; Kulkarni, S. A.; Mhaisalkar, S.; Gratzel, M.; Park, N. G. High Efficiency Solid-State Sensitized Solar Cell-Based on Submicrometer Rutile TiO_2 Nanorod and $CH_3NH_3PbI_3$ Perovskite Sensitizer. *Nano Lett.* **2013**, *13*, 2412−2417.

(7) Gao, X.; Li, J.; Baker, J.; Hou, Y.; Guan, D.; Chen, J.; Yuan, C. Enhanced Photovoltaic Performance of Perovskite $CH_3NH_3PbI_3$ Solar Cells with Freestanding TiO_2 Nanotube Array Films. *Chem. Commun.* **2014**, *50*, 6368−6371.

(8) Burschka, J.; Pellet, N.; Moon, S. J.; Humphry-Baker, R.; Gao, P.; Nazeeruddin, M. K.; Gratzel, M. Sequential Deposition as a Route to High-Performance Perovskite-Sensitized Solar Cells. *Nature* **2013**, *499*, 316−319.

(9) Fakharuddin, A.; Di Giacomo, F.; Palma, A. L.; Matteocci, F.; Ahmed, I.; Razza, S.; D'Epifanio, A.; Licoccia, S.; Ismail, J.; Di Carlo, A.; Brown, T. M.; Jose, R. Vertical TiO_2 Nanorods as a Medium for Stable and High-Efficiency Perovskite Solar Modules. *ACS Nano* **2015**, *9*, 8420−8429.

(10) Xu, Y.; Zhou, M.; Wen, L.; Wang, C.; Zhao, H.; Mi, Y.; Liang, L.; Fu, Q.; Wu, M.; Lei, Y. Highly Ordered Three-Dimensional Ni-TiO_2 nanoarrays as Sodium Ion Battery Anodes. *Chem. Mater.* **2015**, *27*, 4274−4280.

(11) Roy, P.; Berger, S.; Schmuki, P. TiO_2 Nanotubes: Synthesis and Applications. *Angew. Chem., Int. Ed.* **2011**, *50*, 2904−2939.

(12) Sarkar, A.; Jeon, N. J.; Noh, J. H.; Seok, S. I. Well-Organized Mesoporous TiO_2 photoelectrodes by Block Copolymer-Induced Sol−Gel Assembly for Inorganic−Organic Hybrid Perovskite Solar Cells. *J. Phys. Chem. C* **2014**, *118*, 16688−16693.

(13) Wu, W. Q.; Feng, H. L.; Rao, H. S.; Xu, Y. F.; Kuang, D. B.; Su, C. Y. Maximizing Omnidirectional Light Harvesting in Metal Oxide Hyperbranched Array Architectures. *Nat. Commun.* **2014**, *5*, No. 3968.

(14) Mattesini, M.; de Almeida, J. S.; Dubrovinsky, L.; Dubrovinskaia, N.; Johansson, B.; Ahuja, R. Cubic TiO_2 as a Potential Light Absorber in Solar-Energy Conversion. *Phys. Rev. B: Condens. Matter Mater. Phys.* **2004**, *70*, No. 115101.

(15) Tao, J.; Luttrell, T.; Batzill, M. A Two-Dimensional Phase of TiO_2 with a Reduced Bandgap. *Nat. Chem.* **2011**, *3*, 296−300.

(16) Lee, J. S.; You, K. H.; Park, C. B. Highly Photoactive, Low Bandgap TiO_2 Nanoparticles Wrapped by Graphene. *Adv. Mater.* **2012**, *24*, 1084−1088.

(17) Dette, C.; Perez-Osorio, M. A.; Kley, C. S.; Punke, P.; Patrick, C. E.; Jacobson, P.; Giustino, F.; Jung, S. J.; Kern, K. TiO_2 Anatase with a Bandgap in the Visible Region. *Nano Lett.* **2014**, *14*, 6533−6538.

(18) Chen, W.; Wu, Y.; Liu, J.; Qin, C.; Yang, X.; Islam, A.; Cheng, Y.-B.; Han, L. Hybrid Interfacial Layer Leads to Solid Performance Improvement of Inverted Perovskite Solar Cells. *Energy Environ. Sci.* **2015**, *8*, 629−640.

(19) Macak, J. M.; Zlamal, M.; Krysa, J.; Schmuki, P. Self-Organized TiO_2 Nanotube Layers as Highly Efficient Photocatalysts. *Small* **2007**, *3*, 300−304.

(20) Xiao, F. Self-Assembly Preparation of Gold Nanoparticles-TiO_2 Nanotube Arrays Binary Hybrid Nanocomposites for Photocatalytic Applications. *J. Mater. Chem.* **2012**, *22*, 7819−7830.

(21) Xiao, F. Layer-by-Layer Self-Assembly Construction of Highly Ordered Metal-TiO_2 Nanotube Arrays Heterostructures (M/TNTs, M = Au, Ag, Pt) with Tunable Catalytic Activities. *J. Phys. Chem. C* **2012**, *116*, 16487−16498.

(22) Xiao, F. An Efficient Layer-by-Layer Self-Assembly of Metal-TiO_2 Nanoring/Nanotube Heterostructures, M/T-NRNT (M = Au, Ag, Pt), for Versatile Catalytic Applications. *Chem. Commun.* **2012**, *48*, 6538−6540.

(23) Kempa, K.; Kimball, B.; Rybczynski, J.; Huang, Z.; Wu, P.; Steeves, D.; Sennett, M.; Giersig, M.; Rao, D.; Carnahan, D.; et al. Photonic Crystals Based on Periodic Arrays of Aligned Carbon Nanotubes. *Nano Lett.* **2003**, *3*, 13−18.

(24) Foster, S.; John, S. Light-Trapping in Dye-Sensitized Solar Cells. *Energy Environ. Sci.* **2013**, *6*, 2972−2983.

(25) Lan, Y.; Gao, X.; Zhu, H.; Zheng, Z.; Yan, T.; Wu, F.; Ringer, S. P.; Song, D. Titanate Nanotubes and Nanorods Prepared from Rutile Powder. *Adv. Funct. Mater.* **2005**, *15*, 1310−1318.

(26) Shin, H.; Jeong, D. K.; Lee, J.; Sung, M. M.; Kim, J. Formation of TiO_2 and ZrO_2 Nanotubes Using Atomic Layer Deposition with Ultraprecise Control of the Wall Thickness. *Adv. Mater.* **2004**, *16*, 1197−1200.
(27) Knez, M.; Nielsch, K.; Niinistö, L. Synthesis and Surface Engineering of Complex Nanostructures by Atomic Layer Deposition. *Adv. Mater.* **2007**, *19*, 3425−3438.
(28) Li, A. P.; Müller, F.; Birner, A.; Nielsch, K.; Gösele, U. Hexagonal Pore Arrays with a 50−420 nm Interpore Distance Formed by Self-Organization in Anodic Alumina. *J. Appl. Phys.* **1998**, *84*, 6023.
(29) Losic, D., Santos, A., Eds. *Electrochemically Engineered Nanoporous Materials: Methods, Properties and Applications*; Springer Series in Materials Science, Vol. *220*; Springer: 2015; DOI: 10.1007/978-3-319-20346-1.
(30) Zhong, D.; Cai, B.; Wang, X.; Yang, Z.; Xing, Y.; Miao, S.; Zhang, W.-H.; Li, C. Synthesis of Oriented TiO_2 Nanocones with Fast Charge Transfer for Perovskite Solar Cells. *Nano Energy* **2015**, *11*, 409−418.
(31) Lakshmi, B. B.; Dorhout, P. K.; Martin, C. R. Sol-Gel Template Synthesis of Semiconductor Nanostructures. *Chem. Mater.* **1997**, *9*, 857−862.
(32) Kasuga, T.; Hiramatsu, M.; Hoson, A.; Sekino, T.; Niihara, K. Formation of Titanium Oxide Nanotube. *Langmuir* **1998**, *14*, 3160−3163.
(33) Sander, M. S.; Cote, M. J.; Gu, W.; Kile, B. M.; Tripp, C. P. Template-Assisted Fabrication of Dense, Aligned Arrays of Titania Nanotubes with Well-Controlled Dimensions on Substrates. *Adv. Mater.* **2004**, *16*, 2052−2057.
(34) Chu, S. Z.; Wada, K.; Inoue, S.; Todoroki, S. Formation and Microstructures of Anodic Alumina Films from Aluminum Sputtered on Glass Substrate. *J. Electrochem. Soc.* **2002**, *149*, B321−B327.
(35) Foong, T. R.; Sellinger, A.; Hu, X. Origin of the Bottlenecks in Preparing Anodized Aluminum Oxide (AAO) Templates on ITO Glass. *ACS Nano* **2008**, *2*, 2250−2256.
(36) Galstyan, V.; Vomiero, A.; Concina, I.; Braga, A.; Brisotto, M.; Bontempi, E.; Faglia, G.; Sberveglieri, G. Vertically Aligned TiO_2 Nanotubes on Plastic Substrates for Flexible Solar Cells. *Small* **2011**, *7*, 2437−2442.
(37) Jen, H. P.; Lin, M. H.; Li, L. L.; Wu, H. P.; Huang, W. K.; Cheng, P. J.; Diau, E. W. High-Performance Large-Scale Flexible Dye-Sensitized Solar Cells Based on Anodic TiO_2 Nanotube Arrays. *ACS Appl. Mater. Interfaces* **2013**, *5*, 10098−10104.
(38) Fang, M.; Lin, H.; Cheung, H. Y.; Xiu, F.; Shen, L.; Yip, S.; Pun, E. Y.; Wong, C. Y.; Ho, J. C. Polymer-Confined Colloidal Monolayer: A Reusable Soft Photomask for Rapid Wafer-Scale Nanopatterning. *ACS Appl. Mater. Interfaces* **2014**, *6*, 20837−20841.
(39) Fang, M.; Lin, H.; Cheung, H. Y.; Yip, S.; Xiu, F.; Wong, C. Y.; Ho, J. C. Optical Nanoscale Patterning through Surface-Textured Polymer Films. *Adv. Opt. Mater.* **2014**, *2*, 855−860.
(40) Xia, D.; Jiang, Y.-B.; He, X.; Brueck, S. R. J. Titania Nanostructure Arrays from Lithographically Defined Templates. *Appl. Phys. Lett.* **2010**, *97*, No. 223106.
(41) Oskam, G.; Nellore, A.; Penn, R. L.; Searson, P. C. The Growth Kinetics of TiO_2 nanoparticles from Titanium(IV) Alkoxide at High Water/Titanium Ratio. *J. Phys. Chem. B* **2003**, *107*, 1734−1738.
(42) Mor, G. K.; Kim, S.; Paulose, M.; Varghese, O. K.; Shankar, K.; Basham, J.; Grimes, C. A. Visible to near-Infrared Light Harvesting in TiO_2 Nanotube Array-P_3HT Based Heterojunction Solar Cells. *Nano Lett.* **2009**, *9*, 4250−4257.
(43) Tang, H.; Prasad, K.; Sanjinès, R.; Schmid, P. E.; Lévy, F. Electrical and Optical Properties of TiO_2 Anatase Thin Films. *J. Appl. Phys.* **1994**, *75*, 2042−2047.
(44) Xu, X.; Zhai, T.; Shao, M.; Huang, J. Anodic Formation of Anatase TiO_2 Nanotubes with Rod-Formed Walls for Photocatalysis and Field Emitters. *Phys. Chem. Chem. Phys.* **2012**, *14*, 16371−16376.
(45) Jennings, J. R.; Ghicov, A.; Peter, L. M.; Schmuki, P.; Walker, A. B. Dye-Sensitized Solar Cells Based on Oriented TiO_2 Nanotube Arrays: Transport, Trapping, and Transfer of Electrons. *J. Am. Chem. Soc.* **2008**, *130*, 13364−13372.
(46) Xiao, M.; Huang, F.; Huang, W.; Dkhissi, Y.; Zhu, Y.; Etheridge, J.; Gray-Weale, A.; Bach, U.; Cheng, Y.-B.; Spiccia, L. A Fast Deposition-Crystallization Procedure for Highly Efficient Lead Iodide Perovskite Thin-Film Solar Cells. *Angew. Chem.* **2014**, *126*, 10056−10061.
(47) Hua, B.; Wang, B.; Yu, M.; Leu, P. W.; Fan, Z. Rational geometrical design of multi-diameter nanopillars for efficient light harvesting. *Nano Energy* **2013**, *2*, 951−957.

DOI: 10.1021/acsami.6b12474
ACS Appl. Mater. Interfaces 2017, 9, 6265−6272